Electronic Supplementary Information

Mapping the phase-separated state in a 2D magnet

Hinrich Mattiat,[1,§] Lukas Schneider,[1,§] Patrick Reiser,[1] Martino Poggio,[1,*] Pardis Sahafi,[2,#] Andrew Jordan,[2] Raffi Budakian,[2] Dmitry V. Averyanov,[3] Ivan S. Sokolov,[3] Alexander N. Taldenkov,[3] Oleg E. Parfenov,[3] Oleg A. Kondratev,[3] Andrey M. Tokmachev,[3] Vyacheslav G. Storchak[3,*]

[1] *Department of Physics & Swiss Nanoscience Institute, University of Basel, 4056 Basel, Switzerland.*

[2] *Department of Physics and Astronomy & Institute for Quantum Computing, University of Waterloo, Waterloo, ON N2L 3G1, Canada*

[3] *National Research Center "Kurchatov Institute", Kurchatov Sq. 1, 123182 Moscow, Russia.*

[§] Contributed equally to this work

[#] Current affiliation: *National Research Council, Ottawa, ON K1A 0R6, Canada*

Note S1. Nanowire magnetic force microscopy

We describe the motion of the nanowire (NW) tip in each of the two fundamental flexural modes as an independent driven damped harmonic oscillator:[68]

$$m\ddot{x}(t) + \Gamma\dot{x}(t) + kx(t) = F_x(t), \quad (1)$$

where the mode is characterized by the effective mass m, the dissipation Γ, the spring constant k, and is driven by the force component F_x along the mode oscillation direction. The Fourier transform of this equation of motion yields the response of the flexural motion to the driving force:

$$-m\omega^2\tilde{x}(\omega) + i\Gamma\omega\tilde{x}(\omega) + k\tilde{x}(\omega) = \tilde{F}_x(\omega), \quad (2)$$

$$\tilde{x}(\omega) = \left(\frac{1}{m\left({\omega_0}^2 - \omega^2\right) + i\Gamma\omega}\right)\tilde{F}_x(\omega) \quad , \tag{3}$$

where $\omega_0 = \sqrt{k/m}$ is the angular resonance frequency.

The response of each mode can be changed by the interaction of the tip with the sample. For a NW with a magnetic tip, the dominant interactions are with the stray magnetic fields produced by the sample below. In particular, any response in-phase or in quadrature with the NW displacement $x(t)$ results in changes of the resonant frequency or the dissipation. Separating the Fourier transform of the driving force into forces in-phase and in quadrature with the displacement, as well as a force not proportional to the NW motion, we have:

$$-m\omega^2\tilde{x}(\omega) + i\Gamma\omega\tilde{x}(\omega) + k\tilde{x}(\omega) = \alpha_I\tilde{x}(\omega) + i\alpha_Q\tilde{x}(\omega) + \tilde{F}_{x,0}(\omega), \tag{4}$$

$$\tilde{x}(\omega) = \left(\frac{1}{m\left({\omega_0}^2 - \frac{\alpha_I}{m} - \omega^2\right) + i(\Gamma\omega - \alpha_Q)}\right)\tilde{F}_{x,0}(\omega) \quad , \tag{5}$$

where α_I and α_Q are the proportionality constants of the in-phase and quadrature forces with respect to the displacement, respectively.

This transfer function results in a modified angular resonance frequency $\omega_0{}' = \sqrt{{\omega_0}^2 - \frac{\alpha_I}{m}}$ and a modified dissipation $\Gamma' = \Gamma - \frac{\alpha_Q}{\omega}$. In the limit $\alpha_I \ll m{\omega_0}^2 = k$, changes in this angular resonance frequency and dissipation are given by:

$$\Delta\omega_0 = -\frac{\alpha_I}{2m\omega_0}, \tag{6}$$

$$\Delta\Gamma = -\frac{\alpha_Q}{\omega}. \tag{7}$$

Using an approach similar to that used to calibrate MFM tips, we model the force exerted on the tip by a magnetic field by using the so-called point-probe approximation. This approximation models the magnetization distribution of the tip as an effective magnetic monopole moment q_0, ignoring the higher moments.[60] This approximation can be made

because the magnetic tip is magnetized along its axis and because the decay length of the magnetic field from our sample is much shorter than the tip length. In this case, the sample fields only interact with the monopole-like magnetic charge distribution at the closest end of the magnetic tip and not with the opposite charge distribution at the other end. We therefore approximate the force on the NW tip along the NW oscillation direction as:

$$F_x = q_0 B_x, \tag{8}$$

where B_x is the component of the stray magnetic field produced by the sample at the position of the magnetic tip and along the mode oscillation direction. For small oscillations of the NW flexural mode, the tip moves only slightly around its equilibrium position. In this case, we linearly expand B_x as a function of this oscillation around the equilibrium position $x = 0$:

$$F_x = q_0 B_{x,0} + q_0 \left.\frac{dB_x}{dx}\right|_0 x \,. \tag{9}$$

Since the magnetic stray field produced by the magnetization is, in general, not homogenous, $\left.\frac{dB_x}{dx}\right|_0$ contains a term that reflects the spatial gradient of the field G_0. In addition, if the field produced by the NW MFM tip is strong enough, it can induce the sample magnetization to change below it as it oscillates. As the magnetic tip moves above the sample, it modulates the local magnetic field in the sample below, driving changes in its magnetization. In the Fourier domain, these changes will depend on the local magnetic susceptibility of the sample $\chi = \chi' + i\chi''$, which has in general an in-phase χ' and out-of-phase χ'' component. χ' indicates the linear response of the sample magnetization to a change in the local field, while χ'' is related to dissipative processes in the sample magnetization caused by the changing field. These induced changes in local magnetization, in turn, result in x-dependent changes in the stray magnetic field experienced by the MFM tip. As a result, the Fourier transform of the force on the NW tip is:

$$\tilde{F}_x = q_0 \tilde{B}_{x,0} + q_0 G_0 \tilde{x} + q_0 \gamma \chi' \tilde{x} + i q_0 \gamma \chi'' \tilde{x}, \tag{10}$$

where γ is a constant depending on the details of the tip interaction. The first term on the right-hand side of (10) describes the force acting on the MFM tip from an externally applied

magnetic field with Fourier transform $\mathcal{B}_{x,0}$. The second term quantifies the force acting in-phase with the NW oscillation due to the gradient of the sample's time-independent stray field, quantified by the spatial derivative along x, G_0. The terms involving χ' and χ'' account for in- and out-of-phase forces produced by local magnetization dynamics, driven by the MFM tip itself. By comparing the right-hand side of (10) and (4), we see that:

$$\alpha_I = q_0\left(G_0 + \gamma\chi'\right), \tag{11}$$

$$\alpha_Q = q_0\gamma\chi'', \tag{12}$$

$$\Delta\omega_0 = -\frac{q_0\left(G_0 + \gamma\chi'\right)}{2m\omega_0}, \tag{13}$$

$$\Delta\Gamma = -\frac{q_0\gamma\chi''}{\omega}. \tag{14}$$

If as in Fig. 4 of the main text, the sample is magnetized by a large applied field, then the static magnetic field gradient produced by the sample is much larger than the dynamic effect of the tip on the sample, *i.e.* $G_0 \gg \gamma\chi'$. In this case, $\Delta\omega_0 \approx -\frac{q_0 G_0}{2m\omega_0}$ and the measured frequency shift is proportional to the gradient of the static stray magnetic field produced by the sample. If, on the other hand, as in Fig. 5 of the main text, there is no applied field and the sample is not strongly magnetized, the dynamic effect of the tip on the sample can dominate, *i.e.* $\gamma\chi' \gg G_0$. Then, $\Delta\omega_0 \approx -\frac{q_0\gamma\chi'}{2m\omega_0}$. In this case, as shown in Fig. 5 of the main text, $\Delta\omega_0$ and $\Delta\Gamma$ reveal information about the in-phase and out-of-phase magnetic susceptibility of the part of the sample in immediate proximity to the NW MFM tip.

Note S2. Fourier analysis of feature size

In order to analyze the spatial extent of the magnetic structure inhomogeneities present in both the Δf and $\Delta\Gamma$ images, the data points from a 1.7 × 1.7 μm^2 window were subjected to a 2D Fourier transform. Subsequently the data were high-pass filtered and different spatial

frequency components extracted by integrating over all directions with fixed spatial frequency in reciprocal space.

The results are plotted in Fig. S2 for Δf and $\Delta\Gamma$ as a function of the spatial frequency and temperature. Focusing on Δf, the characteristic feature size is roughly between 250 and 500 nm for the whole temperature range although smaller features are also present below 12 K. Focusing on $\Delta\Gamma$, at the onset of the transition many different spatial frequency components are present, ranging from 120 to 900 nm. However, the low spatial frequency components at 580 and 900 nm, exhibit a maximum during the onset of the transition. At the peak in $\Delta\Gamma$ near 10 K, the intensity gradually shifts to higher spatial frequencies with this trend continuing down to lower temperatures.

This analysis is limited by a scan resolution of about 50 nm per pixel. However, it demonstrates the clear differences between the two measurement channels – Δf and $\Delta\Gamma$ – peaked at different temperatures and exhibiting features of different sizes, which are independent of each other.

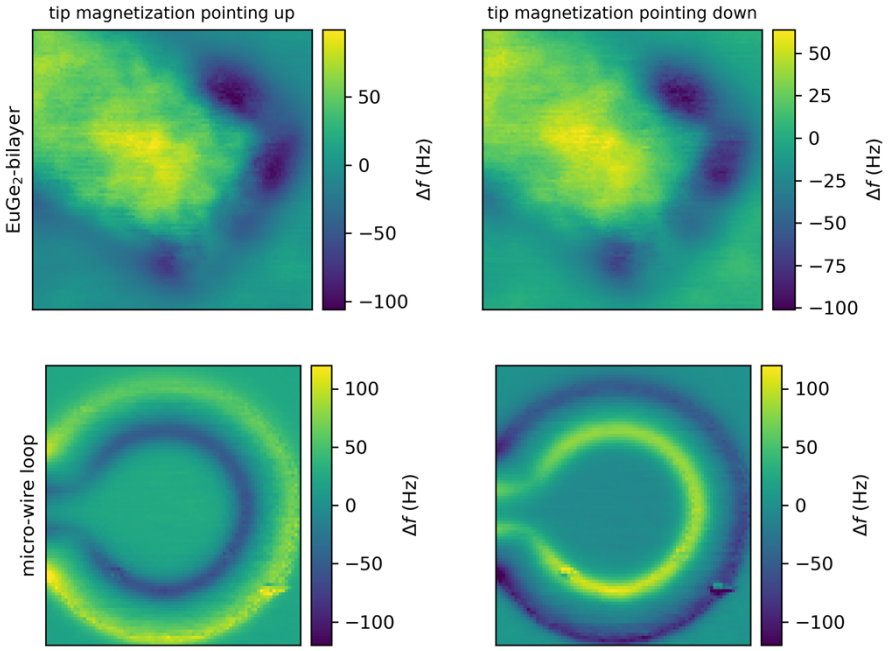

Fig. S1. Top row: $EuGe_2$ bilayer sample imaged at zero field and at $T = 7.3$ K before and after switching the tip magnetization by applying a small reverse field. Bottom row: Au-mircrowire loop with a constant DC current passing through, also imaged before and after switching the tip magnetization. In the second case the contrast is inverted as is expected when imaging the gradient of a static stray magnetic field. However, on the $EuGe_2$ bilayer sample no contrast inversion is observed, making the case for the contrast in Fig. 5a being dominated by the in-phase AC magnetic susceptibility (see Eq. 13).

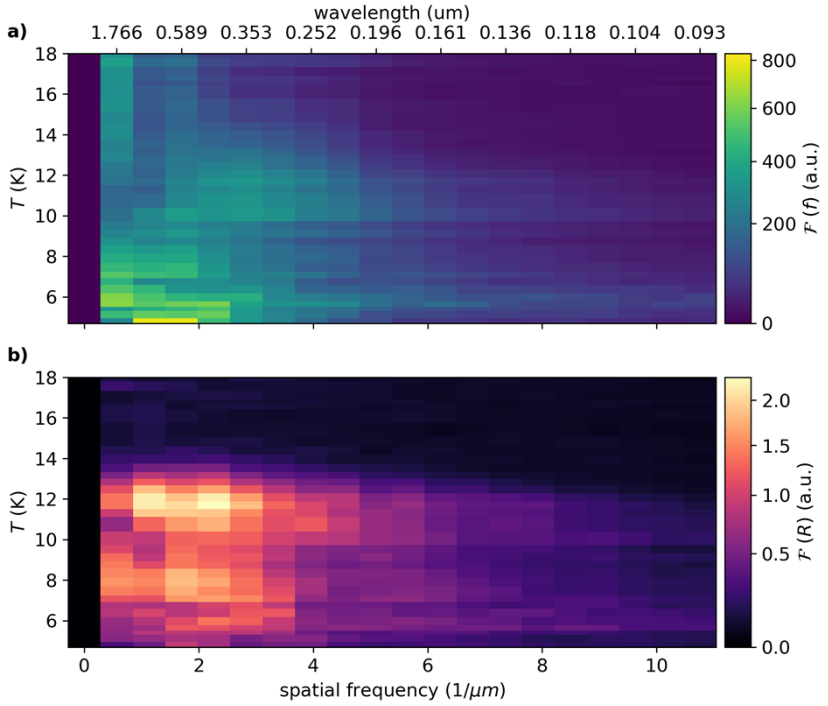

Fig. S2. Fourier analysis of the Δf and $\Delta\Gamma$ images of the inner part of the $EuGe_2$ bilayer sample shown in Figs. 5a and b measured at zero field. Fourier transform of a) the combined frequency shift Δf and b) the dissipation $\Delta\Gamma$, plotted as a function of spatial frequency and temperature. Please note the non-linear color bars that highlight the tails at higher spatial frequencies.